Eng. Sci., 2022, **17**, 319–327

Engineered Science

DOI: https://dx.doi.org/10.30919/es8d625

A Double-layer Carbon Nanotubes/Polyvinyl Alcohol Hydrogel with High Stretchability and Compressibility for Human Motion Detection

Kun Huang,[1] Yufeng Wu,[1] Junchen Liu,[1] Geng Chang,[2] Xuchao Pan,[2,*] Xiaodi Weng,[3,*] Yonggang Wang[1] and Ming Lei[1,*]

Abstract

With the development of technology and the improvement of living standards, hydrogel-based strain sensors have attracted more attention. However, the fabrication of hydrogel strain sensors with desirable mechanical and piezoresistive properties is still challenging. Herein, a double-layer flexible hydrogel sensor is presented, which is made of carbon nanotubes (CNTs) and polyvinyl alcohol (PVA) with high stretchability up to 415% strain and super compressibility to 92% strain, and considerable electrical conductivity (1.11 S m^{-1}). The hydrogel sensors show great linearity throughout the detection range, excellent durability, and stable relative resistance change ($\Delta R/R_0$) during 1000 loading-unloading cycles. These excellent properties are attributed to a new double-layer structural design, *i.e.* a thin conductive sensor layer of CNTs/PVA deposited on a pure strong PVA substrate. Combined with fast response time (508 ms at stretch and 139 ms at compression) and biocompatibility, this new sensor offers great potential as a wearable sensor for epidermal sensing applications such as detecting the bending of human joints, swallowing, breathing, etc. Besides, the CNTs/PVA hydrogel can operate electronic screens due to its internal ions, and even use mechanical signals to modulate light signals. All of these demonstrate the great advantages of the CNTs/PVA hydrogels as strain sensors.

Keywords: Double-layer structure; Strain sensor; High deformability; Fast-response; Human motion detection.
Received: 14 November 2021; Revised: 24 November 2021; Accepted: 25 November 2021.
Article type: Research article.

1. Introduction

Flexible, stretchable, and wearable electronic devices have drawn enormous attention in recent years due to their promising potential in human health monitoring,[1-4] artificial intelligence,[5-7] flexible luminescence devices,[8-10] and electronic skins.[11-13] In particular, wearable strain and pressure sensors that convert external mechanical stimuli into recordable electrical signals, such as resistance,[14] current,[15] and capacitance,[16] have demonstrated several applications in monitoring motion,[17] strain,[18] pressure,[19] and temperature.[20] Generally, flexible sensing materials are fabricated by embedding conductive materials such as metal nanomaterials,[21-27] carbon nanotubes (CNTs),[28] graphene,[29] and conductive polymers[30,31] into the interior or surface of elastomer substrates such as polyurethane (PU),[32,33] melamine sponge,[22] and polydimethylsiloxane (PDMS).[34] The number of conductive channels changes during stretching or compression, resulting in changes in the electrical signal of the devices. Furthermore, to meet the requirements of human motion detection and biosafety at the same time, flexible sensing devices should be biocompatible. In this respect, hydrogels as elastomers have been extensively used in flexible sensors.[35,36]

Among various types of flexible sensors,[37-39] conductive hydrogels have been playing vital roles in strain sensors due to their excellent electrical conductivity,[40] good biocompatibility,[41] and matched mechanical properties with human skin,[42] and have attracted increasing attention. Selecting appropriate materials is the key to fabricating conductive hydrogels and the necessary condition to achieve wearable functions. Among them, polyvinyl alcohol (PVA) is a highly hydrophilic water-soluble polymer, which has gained great attention in the application research of flexible wearable

[1] *State Key Laboratory of Information Photonics and Optical Communications, School of Science, Beijing University of Posts and Telecommunications, Beijing 100876, China.*
[2] *Ministerial Key Laboratory of ZNDY, Nanjing University of Science &Technology, Nanjing, 210094, China.*
[3] *Unit 96911 of PLA, Beijing, 100010, China.*
**E-mail:* mlei@bupt.edu.cn (M. Lei), fefebi@163.com (X. Weng), pxchxc@njust.edu.cn (X. Pan)

hydrogels due to its low toxicity, high mechanical strength, and excellent water absorption. Therefore, PVA is a very competitive material for flexible wearable applications where biocompatibility is required. Over the past few years, various techniques have been developed to incorporate conductive fillers with flexible substrate/matrix to fabricate hydrogel strain sensors, which have achieved great success in human motion detection and bioelectrical signal recording. Among the conductive fillers of hydrogels, CNTs have attracted special attention due to their excellent mechanical properties and high electrical conductivity.[43] It has been proved that the introduction of a suitable amount of CNTs can provide conductive pathways and enhance the mechanical properties of the hydrogel, resulting in unexceptionable durability in practical applications of strain sensors. For instance, Zhang *et al.* presented a stretchable strain and pressure sensor based on PVA, CNTs, and graphene, which exhibited an extremely high elasticity of up to 900% strain with excellent electrical conductivity and strong mechanical pressure.[44,45] Liao *et al.* prepared a wearable, healable, and adhesive epidermal sensor based on single-wall CNTs, PVA, and polydopamine, which exhibited fast self-healing ability with high self-healing efficiency.[46] These all demonstrate the promising potential of the strain sensors of PVA-based and CNTs conductive filler in applications such as human motion detection and physiological signal recording.

Currently, the research on hydrogel sensors based on PVA and CNTs conductive filler focus on the relationship between mechanical properties and material design factors such as PVA concentration, manufacturing technology, and CNTs concentration. One of the major challenges in developing CNTs/PVA-based nanocomposite hydrogel sensors is to find an appropriate method to properly combine PVA and CNTs conductive nanofiller to realize desired mechanical properties and outstanding electrical conductivity. A high concentration of PVA is the key to obtaining high mechanical strength, which enables the hydrogel sensor to withstand greater stress and strain. Nevertheless, a high concentration of PVA is unfriendly to CNTs due to its viscosity, and CNTs can be better dispersed in a low concentration of PVA solution. To overcome this issue, a novel double-layer CNTs/PVA hydrogel sensor has been developed, which consists of a thin, conductive CNTs/PVA layer and a PVA layer with high mechanical properties. The conductive layer is to mix CNTs conductive filler in low concentration PVA solution, which can disperse high-content CNTs more evenly to achieve the purpose of high conductivity. While the substrate is fabricated from a high concentration of PVA, which can provide mechanical support for the entire hydrogel sensor, and a small amount of glycerol, which can increase the stress tolerance of the whole system.

Herein, a double-layer CNTs/PVA hydrogel strain sensor was prepared by the freezing-thawing cycle method, which was composed of a high concentration of PVA substrate and a low concentration of CNTs/PVA sensing layer. The freezing-thawing method was employed, during which crystallization of PVA occurs and the resulting crystallites act as physical cross-links to establish the strong network in the CNTs/PVA hydrogel. The present study also demonstrates that the CNTs/PVA hydrogel was highly stretchable and compressible. The mechanical strength and sensitivity of the CNTs/PVA hydrogel remained stable during 1000 loading-unloading cycles whether it was stretched to 100% or compressed to 30%. In addition, the CNTs/PVA hydrogel can detect a series of human motions, such as bending of joints, swallowing, and breathing, operate electronic screens through internal ions and even utilize mechanical signals to modulate optical signals, which has excellent prospects in wearable devices.

2. Experimental section

2.1 Materials

Polyvinyl alcohol (PVA) with a degree of polymerization ~1750 ± 50 and Glycerol (F.W. = 92.09, AR) were obtained from Sinopharm Chemical Reagent Co. Ltd., China. Carboxyl-functionalized CNTs (diameter = 5-15 nm, length = 10-30 μm) were purchased from XFNANO (Nanjing) Tech. Co. Ltd., China. Sodium dodecyl sulfate (SDS, Mw = 288.38, AR) was obtained from Shanghai Macklin Biochemical Co. Ltd., China. All chemicals were used without further purification.

2.2 Preparation of CNTs/PVA hydrogels

The double-layer CNTs/PVA hydrogels were prepared via a facile and feasible freezing-thawing cycle strategy. Firstly, 1.68 g PVA crystal and 0.516 g glycerol were added to 9.804 mL deionized water, the mixture was heated at 90 ℃ at 700 rpm for 12 h with magnetic stirring until all the PVA was completely dissolved, and 14wt.% PVA solution was prepared; 1.18 g PVA crystal and 0.52 g glycerol were added to 10.3 mL CNTs dispersion (Fig. S1) and stirred at the same speed and temperature for 12 h to fully mix PVA and CNTs, and 10wt.% CNTs/PVA solution was prepared. Secondly, the above two solutions were placed in an environment of 60℃ to eliminate bubbles for further use. Then the PVA solution was put into the mold. After being frozen for 20 mins and thawed for 30 mins, a thin layer of CNTs/PVA solution was poured, which was frozen for 45 mins and thawed for 40 mins. Double-layer CNTs/PVA hydrogels were obtained through three freezing-thawing (F-T) cycles.

2.3 Characterization

Micromorphological images of the CNTs/PVA hydrogels were measured using a field emission scanning electron microscope (FE-SEM, LEO-1530, Zeiss, Germany).

2.4 Mechanical and electrical measurement

Mechanical tests were carried out in a universal mechanical tester (Zwicki-Z1.0, ZwickRoell GmbH & Co.KG, Germany) equipped with 1 kN load cells. For stretching tests, the CNTs/PVA hydrogel was installed in the grips (the bottom grip is stationary and the top grip is mobile), and the movement of

the top grip was controlled by the software, and data were recorded. To calculate the resistance change of the hydrogel during the stretching process, thin sliver sheets were affixed to both ends of the hydrogel as conductive electrodes. And universal mechanical tester was combined with a computer-controlled electrochemical workstation (CHI 660E, CH Instrument, China) with a double electrode system to simultaneously record the current under constant voltage (0.1V) during the mechanical response test. For compression tests, two sliver sheets were fixed on the bottom plate (the bottom plate is stationary and the top plate is mobile) as conductive electrodes to ensure the stability of the current during the experiment. Similarly, the current value of the hydrogel during compression was recorded by the above method. And the relative change in resistance was calculated using the following Equation (1):

$$\frac{\Delta R}{R_0} = \frac{R-R_0}{R_0} \quad (1)$$

where R_0 and R denote the initial resistance and the resistance at a given mechanical stretching or compression, respectively. In addition, the relative resistance change $\Delta R/R_0$ versus strain $\Delta L/L_0$ data were used to calculate the strain sensitivity GF (gauge factor) from Equation (2):

$$GF = \frac{\Delta R/R_0}{\Delta L/L_0} \quad (2)$$

where L_0 and L denote the initial length and the instantaneous length of the sensor in the stretched or compressive state, respectively.

2.5 Detecting human motion sensing

As a proof-of-concept, the potential application of the fabricated CNTs/PVA hydrogel sensor in human motion detection was examined by directly attaching hydrogel sensors to an index finger, wrist, elbow, and knee using adhesive strips, while the electrodes attached to the two ends of samples were connected to an electrochemical workstation for resistance measurement. During the test, the hydrogel sensor was carefully monitored to ensure good adherence to the skin. The resistance change due to the bending of the finger, wrist, elbow, and knee was recorded. The same method was used to detect swallowing, breathing, treading, and pressing. Furthermore, the participants wearing the hydrogel for the wearable devices and biocompatibility experiments learned about the safety of the experiment in advance through training and signed appropriate written informed consent after introducing and understanding the experiment contents.

3. Results and discussion

We, for the sake of obtaining high-performance sensors, developed a new and simple strategy to fabricate CNTs/PVA hydrogels (Fig. 1a). First of all, PVA crystals were added to a mixture of deionized water and glycerol, and magnetically stirred for 12 h to obtain a 14 wt.% PVA aqueous solution. Afterwards, PVA crystals were added to the mixed solution of CNTs dispersion and glycerol, and 10 wt.% CNTs/PVA mixed solution was obtained after fully dissolving. In the next part,

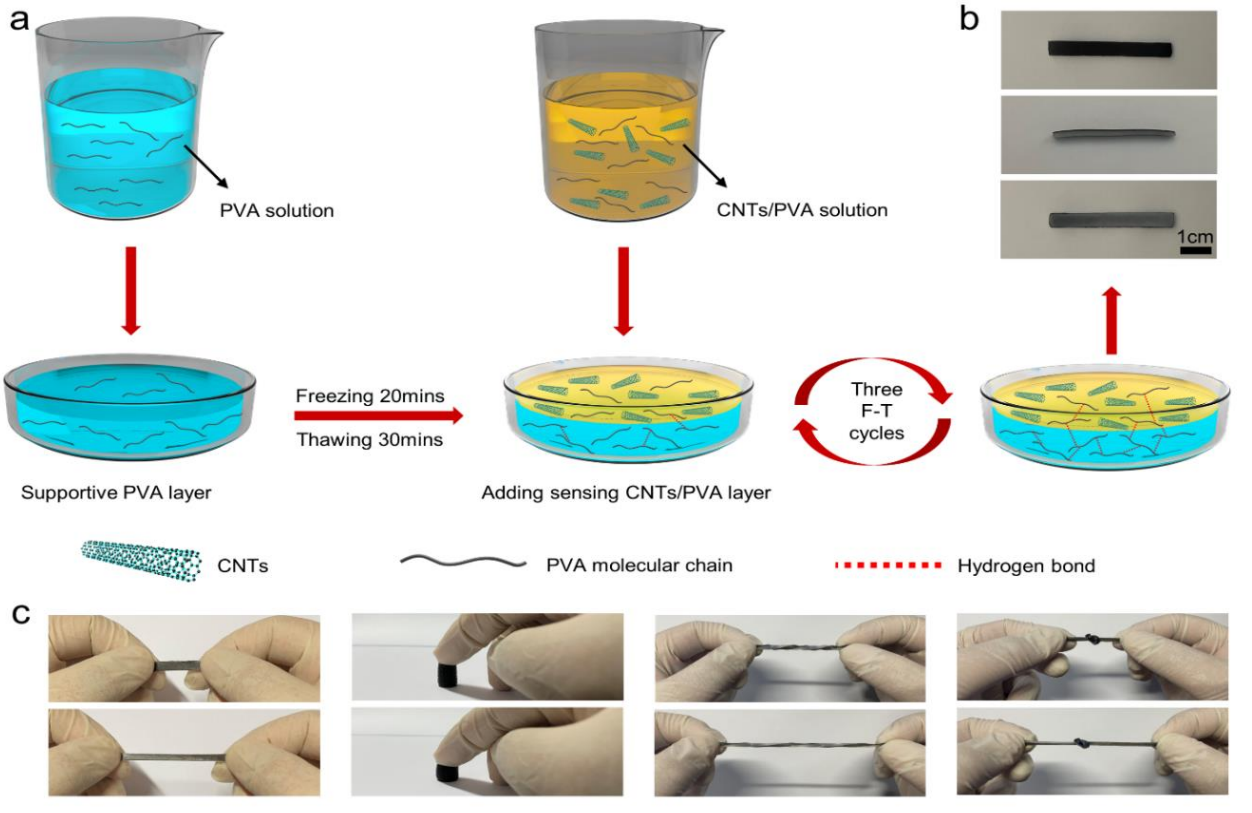

Fig. 1 Fabrication and mechanical properties of the CNTs/PVA hydrogel. (a) Design of the double-layer sensor containing the bottom PVA substrate layer and the top CNTs/PVA sensing layer; (b) Optical diagrams of the CNTs/PVA hydrogel; (c) Photographs demonstrating outstanding stretchability, elasticity, and compressibility of the CNTs/PVA hydrogel.

the PVA solution was poured into the mold for freezing-thawing once, and then the CNTs/PVA mixed solution was poured into the mold as a sensing layer. Finally, CNTs/PVA were poured into the mold as a sensing layer. Finally, CNTs/PVA hydrogels were obtained after the precursor underwent three freezing-thawing cycles. In short, during the freezing-thawing cycles, the enhanced inter-chain hydrogen bonding promoted the formation of PVA crystallites. The stable cross-linked PVA molecular chains maintain intact structure, while unstable hydrogen bonds or unstable crystalline regions can form new physical cross-linked sites and crystalline regions during the next freezing process, and stable gel structures can be obtained after repeated freezing and thawing cycles (Fig. 1b). CNTs/PVA hydrogels can be easily fabricated through molds into sensors of various shapes, such as sheets, cylinders (Fig. S2), *etc*. As shown in Fig. 1c, the CNTs/PVA hydrogel exhibited distinguished deformability to withstand different high-level deformations without fracture, such as stretching, compression, twisted stretching, and knotting stretching. Notably, CNTs/PVA hydrogels can rapidly recover their initial shape after unloading, demonstrating superior elasticity and toughness. The cross-section of the double-layer CNTs/PVA hydrogel sensor presented in Fig. 1b shows that the sensing layer composed of CNTs and PVA is very thin compared to the PVA substrate. Therefore, the mechanical properties of the sensor are mainly dictated by the substrate layer. From the scanning electron microscopy (SEM) images, the surface of the substrate layer was relatively smooth (Fig. 2a), and obvious signs of CNTs can be seen on the surface of the sensing layer (Fig. 2b). Moreover, from the SEM images of the interface of the sensing layer and the substrate in Fig. 2c, we can see that there was a clear boundary, but the two layers were well bonded without any visible delamination.

We then studied the electromechanical properties[47,48] of the CNTs/PVA hydrogel. The CNTs/PVA hydrogel was stretched to different strains (50%, 100%, 150%, 200%, and 250%) with necking phenomenon but no fracture and the initial length could be recovered after unloading with stress relaxation, which showed its high stretchability (Fig. 3a). The stress-strain (σ-ε) curve of the CNTs/PVA hydrogel was tested with a fixed rate of 20 mm min^{-1} (Fig. 3b). The tensile strain of CNTs/PVA hydrogel at break was 415%, and the breaking strength was 777.6 kPa. The σ-ε curve and tensile modulus of another substrate with different PVA concentrations are shown in Figs. S3 and S4. CNTs of different concentrations had a potential effect on conductivity (Fig. S5), but excessive CNTs introduced more defects to the hydrogel, making the CNTs/PVA hydrogel unsustainable for electrical tests at high strain (more than 200%). The cyclic σ-ε curves under different tensile strains (50%, 100%, 150%, 200%, and 250%) were demonstrated in Fig. 3c. Notably, each subsequent loading curve returned to the maximum σ-ε point of the previous cycle and continued the trend of the previous loading curve over all of our measurement ranges, indicating a perfect strain memory effect. Even at the tensile strain of 250%, the σ-ε curve showed a low hysteresis with a hysteresis strain of 3.6%, indicating that the CNTs/PVA hydrogel possessed a good elasticity.

To characterize the long-term electrical stability[49,50] of the CNTs/PVA hydrogel, the relative resistance change ($\Delta R/R_0$) during 1000 loading-unloading processes at 100% strain was recorded. The hydrogel tends to lose part of the water and could not undergo more cycles with a longer testing time, while we added glycerol as a component in the preparation process, which can effectively inhibit or alleviate the water evaporation in the hydrogel. The results showed that the CNTS/PVA hydrogel had good antifatigue conductivity and almost no significant attenuation and fluctuation during the 1000 cycles (Fig. 3e). The 1000 loading-unloading hysteresis curves of the CNTs/PVA hydrogel were also measured synchronously. After being stretched for 1000 cycles, the σ-ε curves almost coincide, indicating the cyclic elastic stability of the CNTs/PVA hydrogel (Fig. S6). The $\Delta R/R_0$ of the CNTs/PVA hydrogel was tested at a speed of 80 mm min^{-1} (500% min^{-1}) at different stretching strains of 50%, 100%,

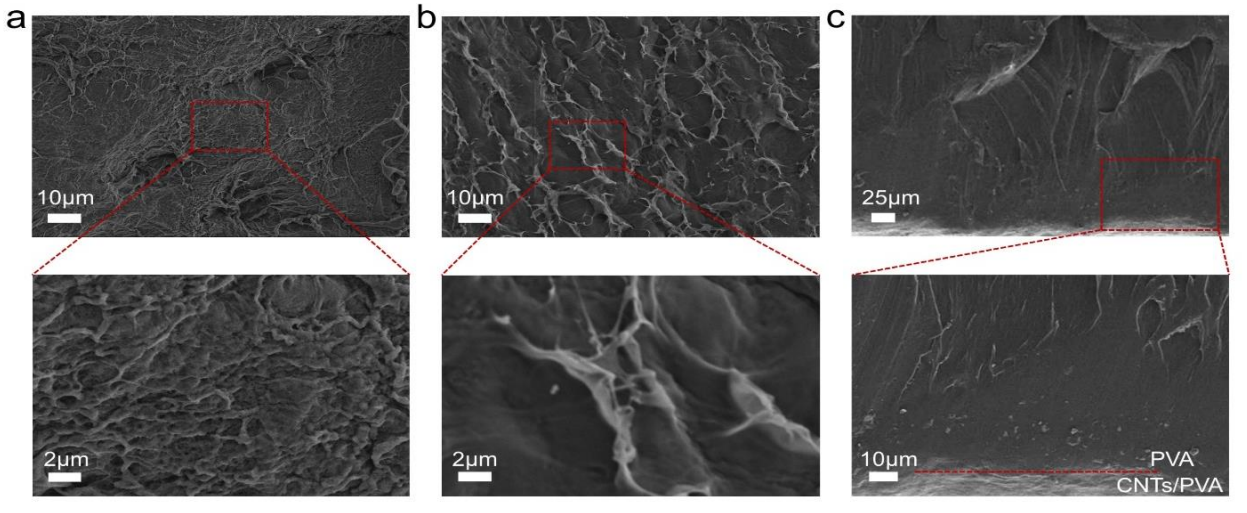

Fig. 2 Microstructure of the CNTs/PVA hydrogel. (a) SEM image of the bottom PVA substrate layer; (b) SEM image of the top CNTs/PVA sensing layer; (c) SEM image of the cross-section view; Dashed lines in (c) indicates the interface of the two layers.

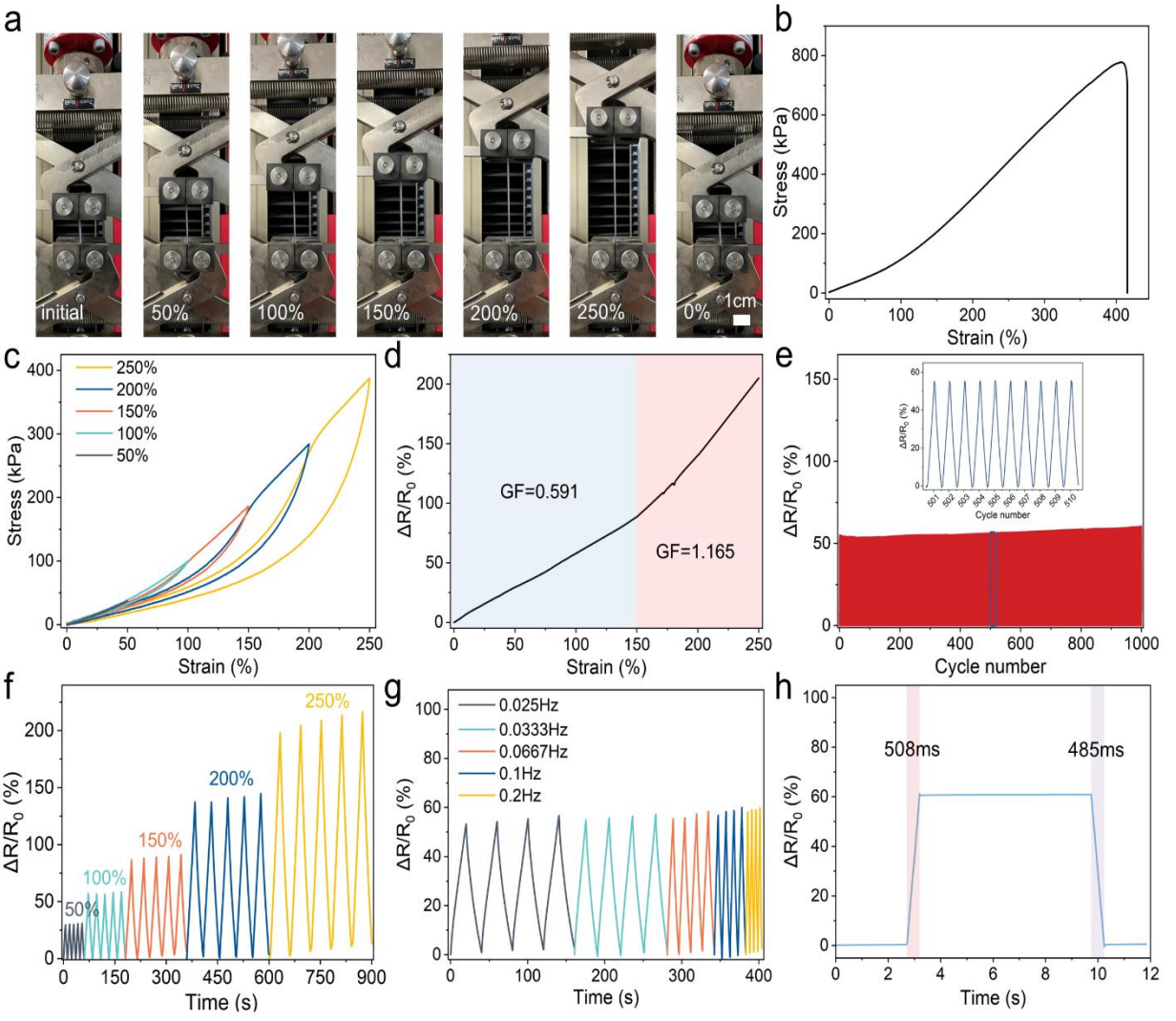

Fig. 3 Mechanical and electrical properties under stretching. (a) Snapshots of the CNTs/PVA hydrogel at the beginning of the test ($\varepsilon = 0$), loaded to a strain of $\varepsilon =$ 50%, 100%, 150%, 200%, 250%, and 0%, respectively; (b) Tensile σ-ε curve of the CNTs/PVA hydrogel; (c) The σ-ε curves of the CNTs/PVA hydrogel at different strains; (d) The gauge factor at a strain of 0-150% and 150-250%; (e) The $\Delta R/R_0$ of the CNTs/PVA hydrogel from 0 to 100% strain for 1000 cycles; (f) The $\Delta R/R_0$ of the CNTs/PVA hydrogel under various tensile strains; (g) The $\Delta R/R_0$ of the CNTs/PVA hydrogel at different frequencies at the strain of 100%; (h) The response time of the sensor during loading and unloading under stretching.

150%, 200%, and 250% (Fig. 3f). The $\Delta R/R_0$ of each strain showed an approximately linear growth trend and remained stable each period, which is very important for the real-time detection of fast and complex movements. At stretching strains of 0-150% and 150-250%, the GF were 0.591 and 1.165, respectively, and it exhibited an increasing trend with the strain (Fig. 3d). When the CNTs/PVA hydrogel was stretched at the strain of 100% and different frequencies (0.025 Hz, 0.0333 Hz, 0.0667 Hz, 0.1 Hz, and 0.2 Hz, respectively), the electrical signal waveforms can remain stable, even though the stress recovery of the hydrogel is different at different speeds (Fig. 3g). The slope of $\Delta R/R_0$ under the same tensile strain increased with higher frequency, indicating the continuous and stable increase of the CNTs/PVA hydrogel resistivity. In addition, the response times of the CNTs/PVA hydrogel during loading and unloading were 508 ms and 485 ms, respectively, which also proved the superiority of the CNTs/PVA hydrogels as sensors (Fig. 3h). All testing results demonstrated that the CNTs/PVA hydrogels as strain sensors had excellent repeatability, stability, durability, and rapid reaction ability.

We further studied the electromechanical performance of the CNTs/PVA hydrogel. The CNTs/PVA hydrogel had no crack or rupture when a 50% compressive strain was applied, and recovered to its initial state after the external strain was removed, indicating its excellent flexibility and elasticity (Fig. 4a). When the compressive strain was set at 92%, the CNTs/PVA hydrogel remained intact and the compressive stress achieved to be 3.06 MPa, showing the impressive super compressibility (Fig. 4b). The σ-ε curves of CNTs/PVA hydrogel under different strains (10%, 20%, 30%, 40%, and 50%) were tested in Fig. 4c. The stress showed an approximately linear trend with the strain at low compressive strains, and the stress increased rapidly at subsequent strains.

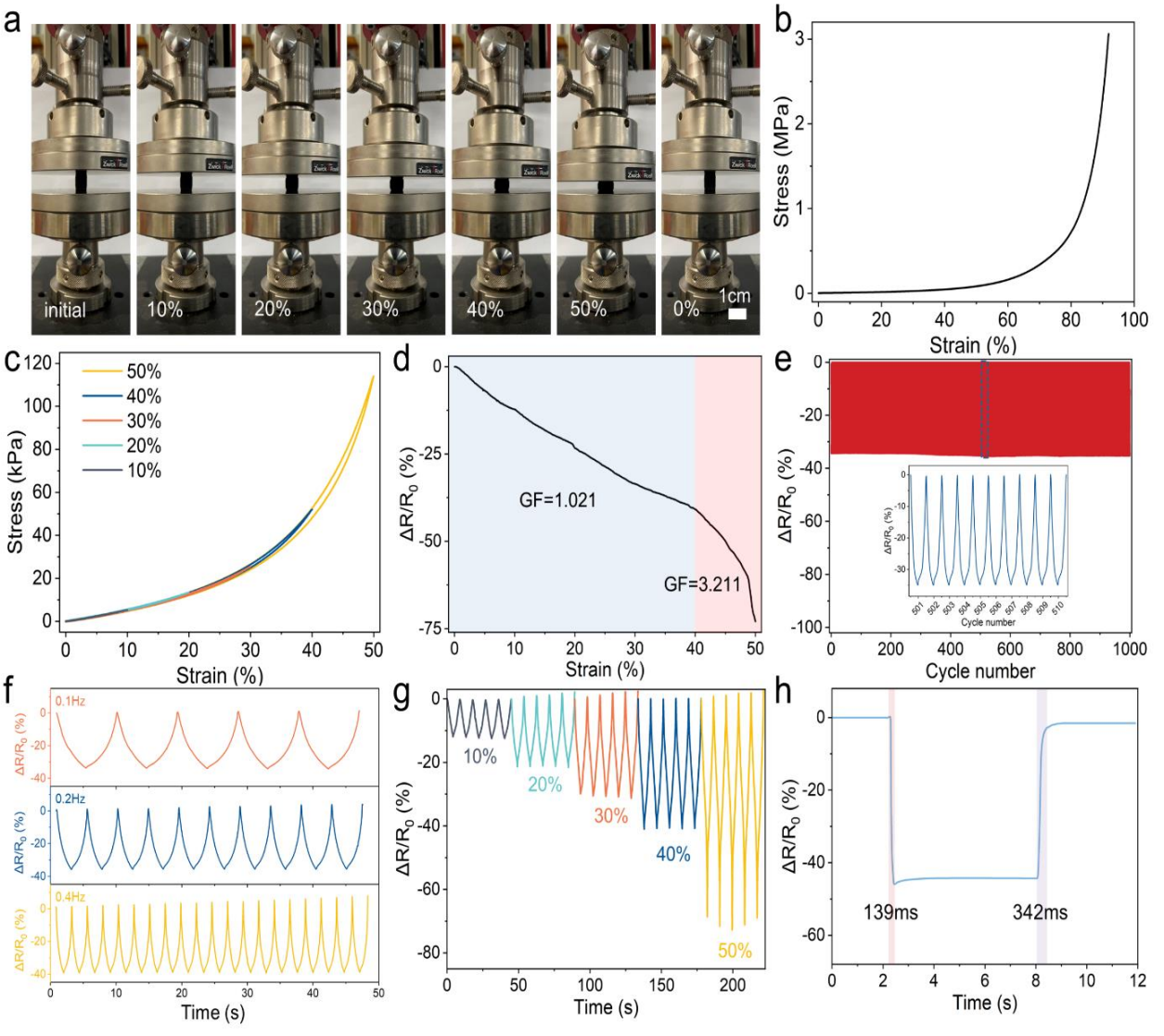

Fig. 4 Mechanical and electrical properties under compressing. (a) Digital photos of the CNTs/PVA hydrogel at different strains; (b) Compressive σ-ε curve of the CNTs/PVA hydrogel; (c) The σ-ε curves of the CNTs/PVA hydrogel at different strains; (d) The gauge factor at a strain of 0-40% and 40-50%; (e) The $\Delta R/R_0$ of the CNTs/PVA hydrogel from 0 to 50% strain for 1000 cycles; (f) The $\Delta R/R_0$ of the CNTs/PVA hydrogel at different frequencies at the strain of 30%; (g) The $\Delta R/R_0$ of the CNTs/PVA hydrogel under various compressive strains; (h) The response time of the sensor during loading and unloading under compressing.

Furthermore, the elastic modulus of the CNTs/PVA hydrogel corresponded to 50.48, 62.06, 79.64, 111.04, and 172.44 kPa at different compressive strains (10%, 20%, 30%, 40%, and 50%) (Fig. S7). The results showed that the elastic modulus increased with increasing strain, which was attributed to the gradual densification of the interior of the materials.

Remarkable anti-softening performance is of great significance to the long-term application of hydrogel-based flexible devices. As shown in Fig. 4e, when the hydrogel was continuously compressed to 50% and released for 1000 cycles, the $\Delta R/R_0$ remained almost constant with minor attenuation and fluctuation, indicating high cyclic stability. To verify the elastic stability of the CNTs/PVA hydrogel, we measured the 1000 loading-unloading σ-ε curves with a compressive strain of 50% (Fig. S8). From the following cycles, each subsequent cycle almost coincided, which was similar to the stretching process, exhibiting good fatigue resistance. At the compressive strain of 30%, the force periodically changed with different frequencies (0.1 Hz, 0.2 Hz, and 0.4 Hz), and the $\Delta R/R_0$ of the CNTs/PVA hydrogel corresponded to 33.91%, 35.53%, and 38.82% (Fig. 4f). This minor electrical signal fluctuation was due to the different stress recovery ability of the CNTs/PVA hydrogel at different frequencies. The $\Delta R/R_0$ of the CNTs/PVA hydrogel under different compressive strains was tested at a fixed frequency, revealing the high repeatability of the electrical signals (Fig. 4g). The GF were 1.021 and 3.211 at compressive strains of 0-40% and 40-50% (Fig. 4d). Moreover, the response times of the CNTs/PVA hydrogel during loading and unloading were 139 ms and 342 ms, respectively, at a compressive strain of 40% (Fig. 4h). These experimental results further demonstrated the advantages of the CNTs/PVA hydrogels as strain sensors.

When the CNTs/PVA was made into fingerstall, the operator can write the word "BUPT" fluently, showing the potential application of the CNTs/PVA hydrogel as electronic skin (Fig. 5a). Furthermore, the outstanding sensing performance on various deformations (elongation, compression, and bend) and pressure will benefit the CNTs/PVA hydrogel as a wearable strain sensor to be utilized for full-range human motion detection. To verify the feasibility, the CNTs/PVA hydrogel-based wearable sensor was fixed on various positions of the human body, and corresponding real-time electrical signals were recorded to monitor different human activities. As demonstrated in Fig. 5b, the CNTs/PVA hydrogel was attached to the finger of the volunteer, and the $\Delta R/R_0$ increased with the increase of the finger's bending angle. Similarly, the hydrogel sensor also produced a periodically sensitive response to the movement of the wrist, elbow, and knee (Fig. 5c). Additionally, the hydrogel sensor can generate different waveforms and distinct $\Delta R/R_0$ values while detecting various physiological electrical signals, including the stretching and tightening of the muscles, such as making a fist, throat vibration during swallowing, and abdominal movement when breathing (Figs. 5d-f). Besides, the wearable hydrogel sensor also can be utilized in daily compressive situations. As shown in Fig. 5g, repeated finger pressing produced stable electrical signals. Also, every gentle treading behavior of the volunteer generated similar waveforms (Fig. 5h). The above results manifested that the CNTs/PVA hydrogel-based sensor possessed excellent electrical stability and reliability for being a wearable device. Particularly, the hydrogel sensor and light-emitting diode (LED) lamp were connected in series into the circuit, and the brightness of the LED changed significantly under the different pressure, indicating the possibility that the CNTs/PVA hydrogel sensor can be used to modulate optical signals by mechanical signals (Fig. 5i).

4. Conclusions

In summary, we developed a very simple, controllable method to create strain sensors with high sensitivity and stability under stretching and compression. Glycerol was uniformly dispersed

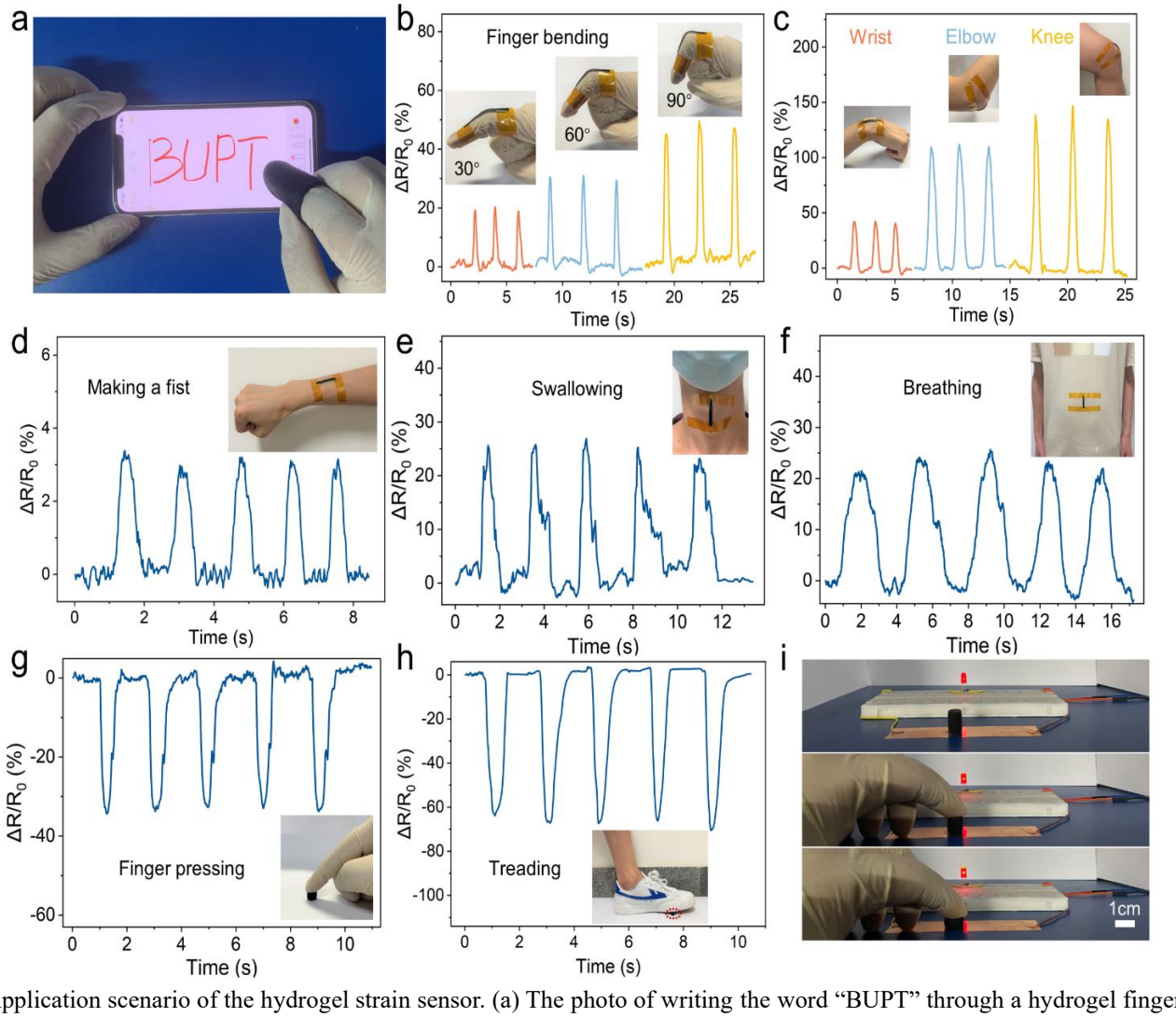

Fig. 5 Application scenario of the hydrogel strain sensor. (a) The photo of writing the word "BUPT" through a hydrogel fingerstall; (b) The $\Delta R/R_0$ for finger's bending at different angles; (c) The $\Delta R/R_0$ for different joints (wrist, elbow, and knee) bending; The $\Delta R/R_0$ for (d) making a fist, (e) swallowing, and (f) breathing; (g) The $\Delta R/R_0$ under finger pressing; (h) The $\Delta R/R_0$ for treading; (i) The changes of LED brightness under different pressure.

inside the CNTs/PVA hydrogel, enhancing mechanical strength and CNTs were added to the sensing layer to ensure electrical conductivity. The CNTs/PVA hydrogel had large stretching (415%) and super compressing (92%) range. In 1000 loading-unloading tests, the $\Delta R/R_0$ maintained at about 55% at a stretching strain of 100%, and the $\Delta R/R_0$ maintained at about 30% at compressing strain of 30%, indicating that the CNTs/PVA has good stability and durability as a strain sensor. Furthermore, this stretchable and compressible property enabled the CNTs/PVA hydrogel to a variety of operating modes and has been demonstrated to successfully detect a wide range of human motions, such as the bending motion of the finger, wrist, elbow, and knee and swallowing and breathing. It also showed its possibility of being an electronic skin. Therefore, this highly stretchable and compressive strain sensor has the potential to be used in a wide range of wearable applications.

Acknowledgments

This study was supported financially by the Fundamental Research Funds for the Central Universities (2021XD-A04-1), the National Natural Science Foundation of China (Nos. 61874014 and 61874013), and the Fund of State Key Laboratory of Information Photonics and Optical Communications (Beijing University of Posts and Telecommunications, P.R. China).

Conflict of interest

There are no conflicts to declare.

Supporting information

Applicable.

References

[1] Z. Li, X. Qi, L. Xu, H. Lu, W. Wang, X. Jin, Z. I. Md, Y. Zhu, Y. Fu, Q. Ni, Y. Dong, *ACS Applied Materials & Interfaces*, 2020, **12**, 42179-42192, doi: 10.1021/acsami.0c12425.

[2] C. M. Boutry, A. Nguyen, Q. O. Lawal, A. Chortos, S. Rondeau-Gagné, Z. Bao, *Advanced Materials*, 2015, **27**, 6954-6961, doi: 10.1002/adma.201502535.

[3] T. Q. Trung, N. E. Lee, *Advanced Materials*, 2016, **28**, 4338-4372, doi: 10.1002/adma.201504244.

[4] Y. Wang, Y. Jia, Y. Zhou, Y. Wang, G. Zheng, K. Dai, C. Liu, C. Shen, *Journal of Materials Chemistry C*, 2018, **6**, 8160-8170, doi: 10.1039/c8tc02702a.

[5] D. Chen, Q. Pei, *Chemical Reviews*, 2017, **117**, 11239-11268, doi: 10.1021/acs.chemrev.7b00019.

[6] M. Ali Darabi, A. Khosrozadeh, R. Mbeleck, Y. Liu, Q. Chang, J. Jiang, J. Cai, Q. Wang, G. Luo, M. Xing, *Advanced Materials*, 2017, **29**, 1700533, doi: 10.1002/adma.201700533.

[7] Y. Yang, Y. Wu, C. Li, X. Yang, W. Chen, *Advanced Intelligent Systems*, 2020, **2**, 1900077, doi: 10.1002/aisy.201900077.

[8] C. C Kim, H. H. Lee, K. H. Oh, J. Y. Sun, *Science*, 2016, **353**, 682-687, doi: 10.1126/science.aaf8810.

[9] X. Qian, Z. Cai, M. Su, F. Li, W. Fang, Y. Li, X. Zhou, Q. Li, X. Feng, W. Li, X. Hu, X. Wang, C. Pan, Y. Song, *Advanced Materials*, 2018, **30**, 1800291, doi: 10.1002/adma.201800291.

[10] D. Yin, N. R. Jiang, Z. Y. Chen, Y. F. Liu, Y. G. Bi, X. L. Zhang, J. Feng, H. B. Sun, *Advanced Optical Materials*, 2020, **8**, 1901525, doi: 10.1002/adom.201901525.

[11] A. Chortos, J. Liu, Z. Bao, *Nature Materials*, 2016, **15**, 937-950, doi: 10.1038/nmat4671.

[12] J. Kang, D. Son, G. J N. Wang, Y. Liu, J. Lopez, Y. Kim, J. Y. Oh, T. Katsumata, J. Mun, Y. Lee, L. Jin, J. B. H. Tok, Z. Bao, *Advanced Materials*, 2018, **30**, 1706846, doi: 10.1002/adma.201706846.

[13] M. Khatib, O. Zohar, W. Saliba, H. Haick, *Advanced Materials*, 2020, **32**, 2000246, doi: 10.1002/adma.202000246.

[14] Y. Liu, H. Fan, K. Li, N. Zhao, S. Chen, Y. Ma, X. Ouyang, X. Wang, *Advanced Materials Technologies*, 2019, **4**, 1900309, doi: 10.1002/admt.201900309.

[15] Y. Park, M. J. Park, J. S. Lee, *Advanced Functional Materials*, 2018, **28**, 1804123, doi: 10.1002/adfm.201804123.

[16] Y. Zhao, J. Cao, Y. Zhang, H. Peng, *Advanced Functional Materials*, 2020, **30**, 1902971, doi: 10.1002/adfm.201902971.

[17] H. Huang, L. Han, Y. Wang, Z. Yang, F. Zhu, M. Xu, *Engineered Science*, 2020, **9**, 60-67, doi: 10.30919/es8d812.

[18] Y. Jiang, M. Liu, X. Yan, T. Ono, L. Feng, J. Cai, D. Zhang, *Advanced Materials Technologies*, 2018, **3**, 1800113, doi: 10.1002/admt.201800113.

[19] P. Wei, X. Yang, Z. Cao, X. L. Guo, H. Jiang, Y. Chen, M. Morikado, X. Qiu, D. Yu, *Advanced Materials Technologies*, 2019, **4**, 1900315, doi: 10.1002/admt.201900315.

[20] W. Lan, Y. Chen, Z. Yang, W. Han, J. Zhou, Y. Zhang, J. Wang, G. Tang, Y. Wei, W. Dou, Q. Su, E. Xie, *ACS Applied Materials & Interfaces*, 2017, **9**, 6644-6651, doi: 10.1021/acsami.6b16853.

[21] S. Lin, X. Bai, H. Wang, H. Wang, J. Song, K. Huang, C. Wang, N. Wang, B. Li, M. Lei, H. Wu, *Advanced Materials*, 2017, **29**, 1703238, doi: 10.1002/adma.201703238.

[22] S. Lin, J. Liu, W. Li, D. Wang, Y. Huang, C. Jia, Z. Li, M. Murtaza, H. Wang, J. Song, Z. Liu, K. Huang, D. Zu, M. Lei, B. Hong, H. Wu, *Nano Letters*, 2019, **19**, 6853-6861, doi: 10.1021/acs.nanolett.9b02019.

[23] H. Cheng, Y. Pan, Q. Chen, R. Che, G. Zheng, C. Liu, C. Shen, X. Liu, *Advanced Composites and Hybrid Materials*, 2021, **4**, 505-513, doi: 10.1007/s42114-021-00224-1.

[24] S. Lin, J. Liu, Q. Wang, D. Zu, H. Wang, F. Wu, X. Bai, J. Song, Z. Liu, Z. Li, K. Huang, B. Li, M. Lei, H. Wu, *Advanced Materials Technologies*, 2020, **5**, 1900761, doi: 10.1002/admt.201900761.

[25] S. Lin, H. Wang, F. Wu, Q. Wang, X. Bai, D. Zu, J. Song, D. Wang, Z. Liu, Z. Li, N. Tao, K. Huang, M. Lei, B. Li, H. Wu, *Npj Flexible Electronics*, 2019, **3**, doi: 10.1038/s41528-019-0050-8.

[26] K. Huang, J. Liu, S. Lin, Y. Wu, E. Chen, Z. He, M. Lei, *Advanced Composites and Hybrid Materials*, 2021, **31**, 2007591, doi: 10.1007/s42114-021-00322-0.

[27] J. Liu, S. Lin, K. Huang, C. Jia, Q. Wang, Z. Li, J. Song, Z. Liu, H. Wang, M. Lei, H. Wu, *Npj Flexible Electronics*, 2020, **4**, 10, doi: 10.1038/s41528-020-0074-0.

[28] B. Cheng, Y. Li, H. Li, H. Li, S. Yang, P. Li, Y. Shang, *Composites Science and Technology*, 2021, **213**, 108948, doi: 10.1016/j.compscitech.2021.108948.
[29] Z. Sun, S. Fang, Y. H. Hu, *Chemical Reviews*, 2020, **120**, 10336-10453, doi: 10.1021/acs.chemrev.0c00083.
[30] H. Liu, Q. Li, S. Zhang, R. Yin, X. Liu, Y. He, K. Dai, C. Shan, J. Guo, C. Liu, C. Shen, X. Wang, N. Wang, Z. Wang, R. Wei, Z. Guo, *Journal of Materials Chemistry C*, 2018, **6**, 12121-12141, doi: 10.1039/c8tc04079f.
[31] N. Wu, W. Du, Q. Hu, S. Vupputuri, Q. Jiang, *Engineered Science*, 2020, **13**, 11-23, doi: 10.30919/es8d1149.
[32] C. Khong Duc, V. P. Hoang, D. Tien Nguyen, T. Thanh Dao, *Polymers*, 2019, **11**, 1247, doi: 10.3390/polym11081247.
[33] X. P. Li, Y. Li, X. Li, D. Song, P. Min, C. Hu, H B. Zhang, N. Koratkar, Z. Z. Yu, *Journal of Colloid and Interface Science*, 2019, **542**, 54-62, doi: 10.1016/j.jcis.2019.01.123.
[34] L. Ma, X. Shuai, Y. Hu, X. Liang, P. Zhu, R. Sun, C. P. Wong, *Journal of Materials Chemistry C*, 2018, **6**, 13232-13240, doi: 10.1039/c8tc04297g.
[35] M. Guo, J. Yan, X. Yang, J. Lai, P. An, Y. Wu, Z. Li, W. Lei, A. T. Smith, L. Sun, *Journal of Materials Chemistry A*, 2021, **9**, 7935-7945, doi: 10.1039/d1ta00112d.
[36] Y. Zhao, B. Zhang, B. Yao, Y. Qiu, Z. Peng, Y. Zhang, Y. Alsaid, I. Frenkel, K. Youssef, Q. Pei, X. He, *Matter*, 2020, **3**, 1196-1210, doi: 10.1016/j.matt.2020.08.024.
[37] X. Chang, L. Chen, J. Chen, Y. Zhu, Z. Guo, *Advanced Composites and Hybrid Materials*, 2021, **4**, 435-450, doi: 10.1007/s42114-021-00292-3.
[38] M. N. Padvi, A. V. Moholkar, S. R. Prasad, N. R. Prasad, *Engineered Science*, 2021, **15**, 20-37, doi: 10.30919/es8d431.
[39] Y. Huang, Y. Luo, H. Liu, X. Lu, J. Zhao, Y. Lei, *Engineered Science*, 2020, **14**, 59-68, doi: 10.30919/es8d1161.
[40] S. Azadi, S. Peng, S. A. Moshizi, M. Asadnia, J. Xu, I. Park, C. H. Wang, S. Wu, *Advanced Materials Technologies*, 2020, **5**, 2000426, doi: 10.1002/admt.202000426.
[41] H. Sun, K. Zhou, Y. Yu, X. Yue, K. Dai, G. Zheng, C. Liu, C. Shen, *Macromolecular Materials and Engineering*, 2019, **304**, 1900227, doi: 10.1002/mame.201900227.
[42] H. Yuk, B. Lu, X. Zhao, *Chemical Society Reviews*, 2019, **48**, 1642-1667, doi: 10.1039/c8cs00595h.
[43] R. Quhe, L. Xu, S. Liu, C. Yang, Y. Wang, H. Li, J. Yang, Q. Li, B. Shi, Y. Li, Y. Pan, X. Sun, J. Li, M. Weng, H. Zhang, Y. Guo, L. Xu, H. Tang, J. Dong, J. Yang, Z. Zhang, M. Lei, F. Pan, J. Lu, *Physics Reports*, 2021, **938**, 1-72, doi: 10.1016/j.physrep.2021.07.006.
[44] Y. Zhang, E. Ren, A. Li, C. Cui, R. Guo, H. Tang, H. Xiao, M. Zhou, W. Qin, X. Wang, L. Liu, *Journal of Materials Chemistry B*, 2021, **9**, 719-730, doi: 10.1039/d0tb01926g.
[45] K. Bi, Q. Wang, J. Xu, L. Chen, C. Lan, M. Lei, *Advanced Optical Materials*, 2021, **9**, 2001474, doi: 10.1002/adom.202001474.
[46] M. Liao, P. Wan, J. Wen, M. Gong, X. Wu, Y. Wang, R. Shi, L. Zhang, *Advanced Functional Materials*, 2017, **27**, 1703852, doi: 10.1002/adfm.201703852.
[47] M. Alsadat Kashfipour, N. Mehra, R. S. Dent, J. Zhu, *Engineered Science*, 2020, **8**, 11-18, doi: 10.30919/es8d508.
[48] N. Pattar, S. F. Patil, *Advanced Composites and Hybrid Materials*, 2019, **2**, 571-585, doi: 10.1007/s42114-019-00119-2.
[49] H. Sun, Z. Fang, T. Li, F. Lei, F. Jiang, D. Li, Y. Zhou, D. Sun, *Advanced Composites and Hybrid Materials*, 2019, **2**, 407-422, doi: 10.1007/s42114-019-00100-z.
[50] J. Cai, W. Xu, Y. Liu, Z. Zhu, G. Liu, W. Ding, G. Wang, H. Wang, Y. Luo, *Engineered Science*, 2018, **5**, 21-29, doi: 10.30919/es8d669.

Author Information

Kun Huang *is a graduate student in the School of Science, Beijing University of Posts and Telecommunications, China. He achieved his Bachelor degree in 2019 from Beijing Jiaotong University, China. His research focuses on flexible wearable electronic devices based on one-dimensional nanometer materials.*

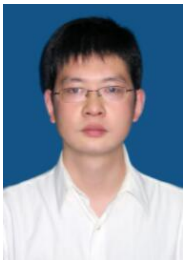

Ming Lei *received his M.D. at State Key Laboratory of Materials Composites and Advanced Technology, Wuhan University of Technology in 2004. Then, he received his Ph.D. from the Laboratory of Nanophysics and Devices, Institute of Physics, Chinese Academy of Sciences in 2007. He worked as a postdoctoral fellow at The Hong Kong University of Science and Technology (2007-2008) and the Chinese University of Hong Kong (2009-2010). He is now a professor and doctoral supervisor of the School of Science, Beijing University of Posts and Telecommunications. He has long been engaged in the preparation of low dimensional nano materials, photoelectric properties and device applications.*